J. Phys. B: At. Mol. Phys. **18** (1985) 955-966. Printed in Great Britain

Electron impact excitation of He-like ions

N R Badnell

Department of Applied Mathematics and Theoretical Physics, Silver Street, Cambridge, CB3 9EW, England

Received 18 June 1984, in final form 5 September 1984

Abstract. The electron impact excitation of He-like ions is studied using an equivalent-electron frozen-core approximation that was developed in an earlier paper on He. The resulting collision equations are solved using a five-state Coulomb exchange distorted-wave approximation that includes the dominant monopole exchange distorting potential exactly. Results are presented for scaled total collision strengths for all inelastic transitions between the 1^1S, 2^3S, 2^1S, 2^3P and 2^1P states of Li^+, Be^{2+}, B^{3+}, C^{4+}, N^{5+}, O^{6+}, Ne^{8+}, Mg^{10+}, Si^{12+}, Ca^{18+} and Fe^{24+}, as well as for the infinite Z limit, for incident electron energies from threshold up to $4.0Z^2$ Ryd. The present results are in good agreement with those of close-coupling and distorted-wave calculations by other workers for transitions from the ground state in O^{6+}.

1. Introduction

A large amount of collision data for He-like ions is required in the study of laboratory and astrophysical plasmas. There have been a few close-coupling calculations; van Wyngaarden *et al* (1979) carried out a five-state calculation and gave results for transitions from the ground state in Li^+, C^{4+}, O^{6+} and Si^{12+}. Five- and eleven-state close-coupling calculations, using the R-matrix method, have been carried out for O^{6+} by Kingston and Tayal (1983) and Tayal and Kingston (1984b) and for C^{4+} and Mg^{10+} by Tayal and Kingston (1984a). Comprehensive calculations have been carried out for transitions from the ground state using the Coulomb-Born and Coulomb-Oppenheimer approximations, and variants thereof. For example, Bely's modification of the Ochkur-Rudge approximation has been investigated by Tully (1980) and Nakazaki and Hashino (1982), but results for the $1^1S \rightarrow n\,^3S$ and $n\,^3D$ transitions were not particularly good. Distorted-wave calculations which treat exchange as a perturbation have been carried out by Steenman-Clark and Faucher (1984) for the $1^1S \rightarrow 2^3S$ transition in O^{6+}, Mg^{10+}, Ca^{18+} and Fe^{24+} and by Pradhan *et al* (1981a), using a five-state expansion, for a number of ions between Be^{2+} and Fe^{24+}. Details of earlier calculations may be found in the review by Henry (1981).

All calculations to date have treated the collision problem explicitly as a three-electron problem and consequently require very accurate atomic wavefunctions to be reliable. Recently (see Badnell 1984, hereafter referred to as III) we have shown by using an equivalent-electron frozen-core approximation that we can reduce the exact three-electron collision equations to a form similar to those for a two-electron problem. This reduces the complexity of the collision problem considerably and enables one to use simple atomic wavefunctions.

0022-3700/85/050955+12$02.25

In this paper we are concerned only with background collision strengths. Pradhan *et al* (1981a, b), like Kingston and Tayal (1983) and Tayal and Kingston (1984a, b), have investigated the resonance structure below the $n = 2$ and $n = 3$ levels and its effect on effective collision strengths, which can be significant. Further discussion of resonances is given by Pradhan (1983b), Steenman-Clark and Faucher (1984) and Trefftz (1983).

In § 2 we provide a brief resumé of the theory and in § 3 we give details of the atomic wavefunctions used. In § 4 we present our results and compare them with those of other authors for transitions from the ground state in O^{6+}. Atomic units are used throughout except for energies which are in rydbergs.

2. Theory

The present approach is based on the assumption that there is no *a priori* reason for using exact atomic wavefunctions in the three-electron collision problem. Given the approximations that need to be made to the exchange term to render the problem tractable (see III), we need only use atomic wavefunctions that are a degree more accurate than the solution of the collision equations. To do this we make two physical approximations. Firstly we use for the 1s core orbital that corresponding to equivalent $1s^2$ electrons while the valence orbital, which is relatively insensitive to the core used, is taken to be that given by a simple Hartree frozen-core approximation. The resulting orthogonality of the core and valence orbitals enables the exact three-electron collision equations to be reduced to a form similar to that for a two-electron problem. The only dependence on the core orbital is via the frozen-core potential which we are free to adjust so that the valence orbitals give the 'exact' value of the $1^1S \rightarrow 2^1P$ line strength (see III, § 3 for further details). We wish to stress that the collision equations we use are thus consistent with our choice of simple atomic wavefunctions. The second approximation we make is to solve the collision equations using a five-state Coulomb exchange distorted-wave approximation which includes the dominant monopole exchange distorting potential exactly (CEDW2, see Badnell 1983a, hereafter referred to as I). Note that this approach gave overall good results for He (see III).

As the residual charge on the ion increases, the exact treatment of the monopole exchange distorting potential becomes less important for the low-lying states that we are considering in this paper. However, the simple form that we have developed for the collision equations is useful for all stages of ionisation.

We expect that our neglect of higher states on using a five-state expansion will mean that our results for the $1^1S \rightarrow 2^1S$ transition will be an overestimate at all energies. Also, our treatment of coupling as perturbation can be expected to affect our results for transitions between the $n = 2$ states at low energies. The errors due to these two approximations will decrease as Z increases. However, as Z increases errors due to the neglect of relativistic effects can become important for spin-forbidden transitions and this is discussed in more detail later. Otherwise, the present method is expected to be reliable for all transitions at all energies.

3. Bound-state wavefunction

We take the valence orbital for the ion to be that given by a Hartree frozen-core approximation and use a hydrogenic core with screening parameter ζ chosen in the

Table 1

Ion	α	$Z^2\sigma^2$		Ion	α	$Z^2\sigma^2$	
		$1^1S\rightarrow 2^1P$	$2^wS\rightarrow 2^wP$†			$1^1S\rightarrow 2^1P$	$2^wS\rightarrow 2^wP$†
Li^+	0.6775	0.8984	17.80	Ne^{8+}	0.642	1.067	10.69
Be^{2+}	0.661	0.9709	14.53	Mg^{10+}	0.635	1.075	10.36
B^{3+}	0.654	1.008	13.02	Si^{12+}	o.630	1.080	10.14
C^{4+}	0.652	1.030	12.15	Ca^{18+}	0.630	1.090	9.775
N^{5+}	0.650	1.045	11.59	Fe^{24+}	0.630	1.095	9.586
O^{6+}	0.650	1.055	11.20	$Z=\infty$	—	1.1097	9.000

† $w=1$ or 3.

way which was discussed in III (§ 3.2). The scaled quantity $\alpha=\zeta/Z$, which is a slowly varying function of the nuclear charge, is given in table 1 for the ions considered in this paper. Also shown are the corresponding values of

$$Z^2\sigma^2(i\rightarrow j)=\frac{Z^2S(i,j)}{\omega_i l_>(2l_j+1)} \tag{3.1}$$

where S is the line strength, ω_i is the statistical weight of the initial state while l_j refers to the final state and $l_>=1$ for transitions $S\rightarrow P$. Note that the values of $\sigma^2(2^wS\rightarrow 2^wP)$ are independent of the spin multiplicity w since we are using a Hartree frozen-core approximation (see III for further details).

For $Z\leqslant 10$ the value of $Z^2\sigma^2(1^1S\rightarrow 2^1P)$ differs by no more than one in the last decimal place from the accurate results of Weiss (1967). For $12\leqslant Z\leqslant 26$, the value that we give for $Z^2\sigma^2$ is that which we interpolated from the values for $Z\leqslant 10$ and for the infinite Z limit. The frozen-core potential, like all short-range potentials, scales as $1/Z$ so in the infinite Z limit the valence orbitals become hydrogenic. Thus as Z increases, $Z^2\sigma^2$ becomes less sensitive to α and in the infinite Z limit the choice of α is arbitrary.

4. Results and discussion

4.1. Transitions from the ground state in O^{6+}

For transitions from the ground state in O^{6+}, we find that treating exchange completely as a perturbation (CEDW1, see I) gives results that differ by less than 5% from those of the CEDW2 approximation and that treating higher multipole exchange potentials exactly (CEDW3, see Badnell 1983b, hereafter referred to as II) gives results that differ by less than 3% from those of the CEDW2 approximation.

Our results are presented in the form of graphs in which we plot a scaled collision strength Y against the (dimensionless) scaled energy X (as in III). We also scale the collision strength Ω in the nuclear charge ($Z=8$) and replace X by $1-X$ so that threshold is now at $X=0$ and $X=1$ corresponds to the infinite energy limit. Thus, for the $1^1S\rightarrow 2^1P$ transition we plot $X=1-1/\ln(k_f^2/c_1+e)$ and $Y=Z^2\Omega/\ln(k_f^2/c_2+c_3)$, for the $1^1S\rightarrow 2^1S$ transition we plot $X=1-1/(k_f^2/c_1+1)$ and $Y=Z^2\Omega$, and for the $1^1S\rightarrow 2^3S$ and $1^1S\rightarrow 2^3P$ transitions we plot $X=1-1/(k_f^2/c_1+1)$ and $Y=Z^2\Omega(k_f^2/c_2+c_3)^2$. k_f^2 is the energy of the electron scattered off the final state and the

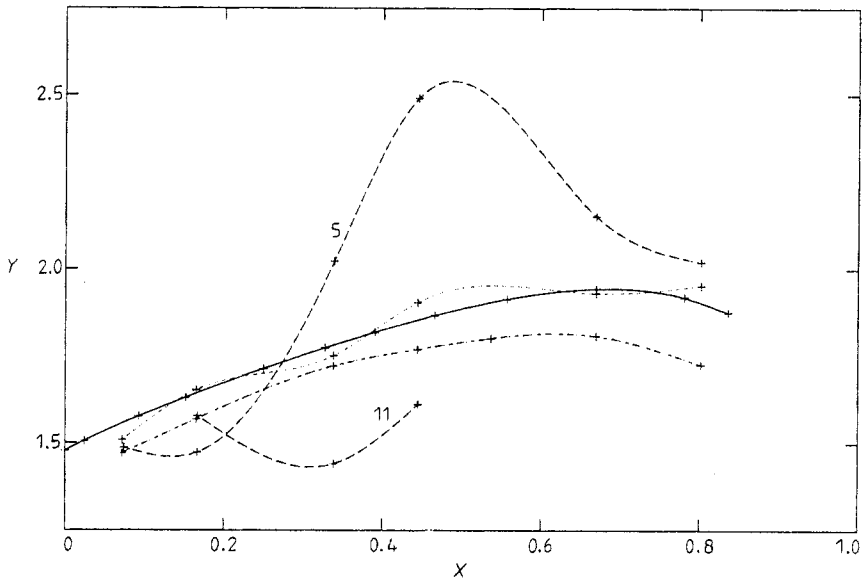

Figure 1. Scaled total collision strengths for the $1^1S \rightarrow 2^3P$ transition in O^{6+}. ——, five-state CEDW2; · · · ·, 5DW (Pradhan *et al* 1981a); – · – · –, 5CC (van Wyngaarden *et al* 1979); – – –, five- and eleven-state R matrix (Kingston and Tayal 1983). $c_1 = 0.65\,Z^2$ Ryd $= c_2$, $c_3 = 1$.

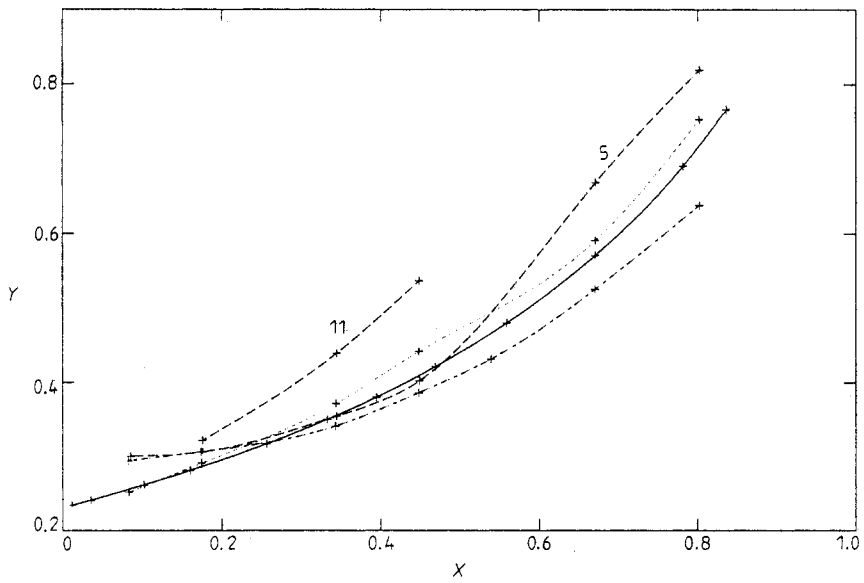

Figure 2. Scaled total collision strengths for the $1^1S \rightarrow 2^3S$ transition in O^{6+}. ——, five-state CEDW2; · · · ·, 5DW (Pradhan *et al* 1981a); – · – · –, 5CC (van Wyngaarden *et al* 1979); – – –, five- and eleven-state R matrix (Kingston and Tayal 1983). $c_1 = 0.65\,Z^2$ Ryd $= c_2$, $c_3 = 1$.

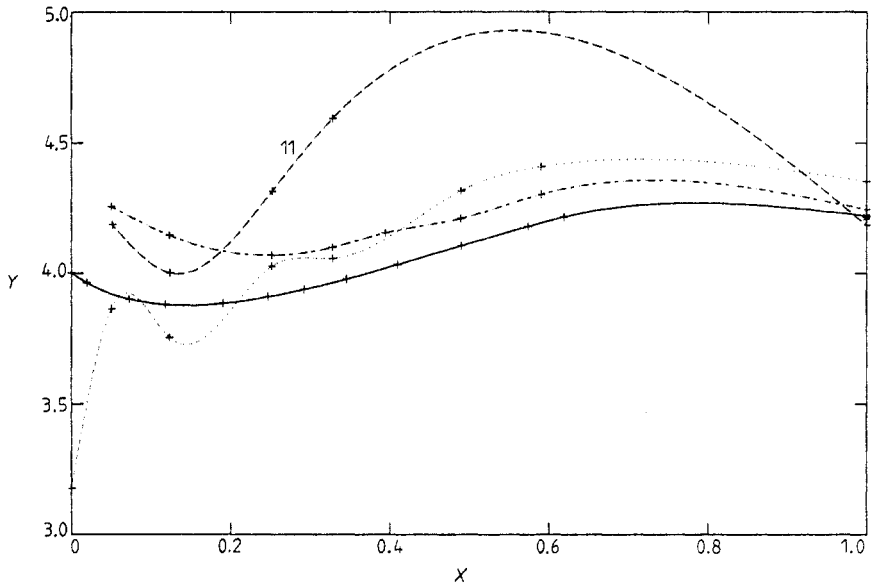

Figure 3. Scaled total collision strengths for the $1^1S \rightarrow 2^1P$ transition in O^{6+}. ——, five-state CEDW2; · · · ·, 5DW (Pradhan *et al* 1981a); – · – · –, 5CC (van Wyngaarden *et al* 1979); – – –, eleven-state R matrix (Tayal and Kingston 1984b); *, 'exact' limit point (Weiss 1967). $c_1 = 0.3\ Z^2$ Ryd, $c_2 = 0.65\ Z^2$ Ryd, $c_3 = 1.343$

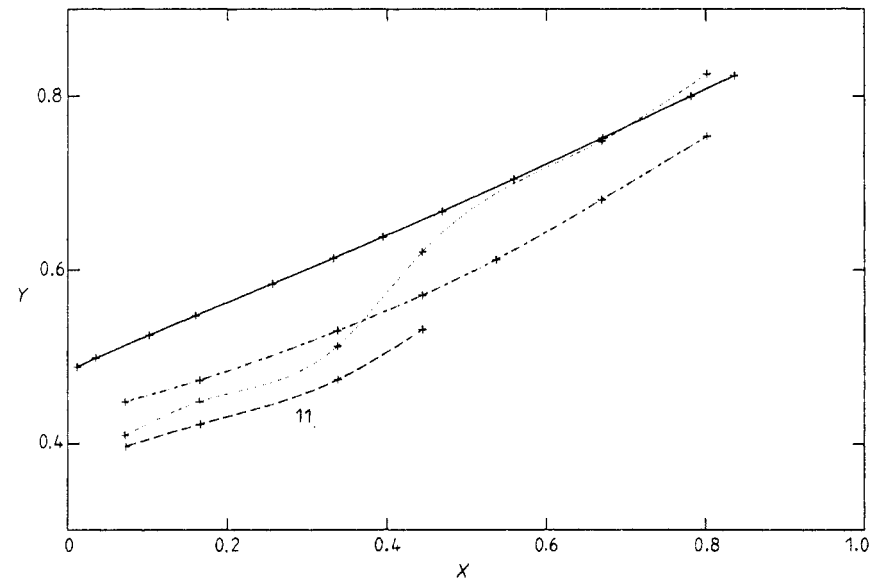

Figure 4. Scaled total collision strengths for the $1^1S \rightarrow 2^1S$ transition in O^{6+}. ——, five-state CEDW2; · · · ·, 5DW (Pradhan *et al* 1981a); – · – · –, 5CC (van Wyngaarden *et al* 1979); – – –, eleven-state R matrix (Tayal and Kingston 1984b). $c_1 = 0.65\ Z^2$ Ryd $= c_2$, $c_3 = 1$.

values used for the constants c_i are given in the captions. A cubic spline was fitted to the N original data points with knots at $i = 2, \ldots, N-1$ and vanishing second-order derivatives at the end points (see e.g. Powell 1981); the original points are marked '+'.

In figures 1-4 we compare our five-state CEDW2 results for the background collision strengths with those obtained by several other groups using a variety of approximations.

For the $1^1S \rightarrow 2^3P$ transition (figure 1) we see that our results are in close agreement with those of the five-state distorted-wave (5DW) calculation by Pradhan *et al* (1981a). There is also good agreement with the five-state close-coupling (5CC) calculation of van Wyngaarden *et al* (1979). The results of the R-matrix calculation of Kingston and Tayal (1983), in particular the five-state, are in poor agreement with the present results. As with He, the bound-bound terms in the eigenfunction expansion of the R-matrix approximation give rise to pseudo-resonances for a wide range of energies above the highest excitation threshold. The referee points out that the $1^1S \rightarrow 2^3P$ five-state R-matrix collision strengths of Kingston and Tayal (1983) have a pseudo-resonance at about 60 Ryd ($X = 0.30$) and that this had an influence on the results at 63 and 75 Ryd ($X = 0.33$ and 0.44) but not at other tabulated energies. Kingston and Tayal (1983) used a smoothing procedure developed by Burke *et al* (1981) that averages the T matrix over the pseudo-resonances. To extract the exact T matrix the averaging procedure of Burke *et al* (1981) requires that the basis of L^2 integrable functions be complete. Kingston and Tayal (1983) use only those L^2 integrable functions that arise from forming the bound-bound terms in the eigenfunction expansion. The question as to whether a large enough L^2 basis has been used to ensure the convergence of the averaging procedure appears not to have been answered. Nevertheless, Burke *et al* (1981) believe that these averaged results are likely to be better than those which take no account of the higher states.

For the $1^1S \rightarrow 2^3S$ transition (figure 2) we see that there is broad agreement between the results shown. However, at low energies, where coupling is important, there is a distinct separation of results into two groups: those of distorted-wave calculations (this paper and Pradhan *et al* 1981a) are as much as 20% below those of the five-state close-coupling calculations (Kingston and Tayal 1983, van Wyngaarden *et al* 1979).

For the $1^1S \rightarrow 2^1P$ transition (figure 3) we also include the 'exact' value of Y at $X = 1$, obtained using the oscillator strength of Weiss (1967). This is the value that the CEDW2 results tend to. We see that in general the results are dominated by their $\ln k^2$ dependence from quite low energies, however, this is not true of the eleven-state R-matrix results of Tayal and Kingston (1984b).

For the $1^1S \rightarrow 2^1S$ transition (figure 4) we see that there is fairly good agreement between the four sets of results, although the CEDW2 results probably still overestimate the collision strength (see III for the case of He).

4.2. The He isoelectronic sequence

In table 2 we present our results for the scaled total collision strengths for all inelastic transitions between the 1^1S, 2^3S, 2^1S, 2^3P and 2^1P states of selected He-like ions from Li^+ to Fe^{24+}, as well as for the infinite Z limit. These were obtained using the CEDW2 approximation with a screened hydrogenic Hartree frozen core adjusted to lead to the 'exact' non-relativistic value of the $1^1S \rightarrow 2^1P$ line strength. k_f^2 is the energy of the free electron scattered off the final state. As we move from Li^+ along the He isoelectronic sequence the scaled total collision strengths converge smoothly to the finite values of the infinite Z limit, except for the $2^1S \rightarrow 2^1P$ and $2^3S \rightarrow 2^3P$ transitions which diverge

Table 2. Scaled total collision strengths $Z^2\Omega$ for transitions in He-like ions.

Ion	k_f^2/Z^2	$1^1S \rightarrow 2^3S$	$1^1S \rightarrow 2^1S$	$2^3S \rightarrow 2^1S$	k_f^2/Z^2	$1^1S \rightarrow 2^3P$	$1^1S \rightarrow 2^1P$	$2^3P \rightarrow 2^1P$	$2^3S \rightarrow 2^1P$	$2^1S \rightarrow 2^3P$	$2^3S \rightarrow 2^3P$	$2^1S \rightarrow 2^1P$
Li^+	1.591−2†	2.43−1	4.45−1	6.43	0	7.97−1	7.73−1	3.71+1	1.49+1	9.72	3.26+2	9.48+1
	5.961−2	2.08−1	4.87−1	4.97	4.370−2	1.06	7.69−1	3.96+1	8.22	7.89	5.50+2	1.76+2
	1.596−1	1.57−1	5.69−1	1.92	1.437−1	1.09	1.02	1.88+1	3.52	3.50	8.03+2	2.65+2
	2.596−1	1.40−1	6.26−1	9.67−1	2.437−1	8.92−1	1.38	9.48	1.83	1.81	9.36+2	3.11+2
	3.596−1	1.26−1	6.68−1	5.90−1	3.437−1	7.16−1	1.74	5.50	1.08	1.08	1.02+3	3.40+2
	4.596−1	1.14−1	7.00−1	4.00−1	4.437−1	5.79−1	2.08	3.55	7.08−1	7.06−1	1.09+3	3.62+2
	5.596−1	1.03−1	7.25−1	2.90−1	5.437−1	4.76−1	2.40	2.46	4.98−1	4.96−1	1.14+3	3.79+2
	7.096−1	8.96−2	7.53−1	1.95−1	6.937−1	3.63−1	2.83	1.57 /	3.22−1	3.21−1	1.20+3	3.99+2
	9.596−1	7.17−2	7.86−1	1.15−1	9.437−1	2.44−1	3.46	8.73−1	1.83−1	1.83−1	1.27+3	4.24+2
	1.460	4.81−2	8.24−1	5.38−2	1.444	1.29−1	4.48	3.81−1	8.30−2	8.29−2	1.38+3	4.59+2
	2.460	2.56−2	8.57−1	2.02−2	2.444	5.24−2	5.95	1.34−1	3.05−2	3.05−2	1.50+3	5.00+2
	3.460	1.57−2	8.71−1	1.05−2	3.444	2.77−2	7.01	6.74−2	1.57−2	1.57−2	1.58+3	5.26+2
Be^{2+}	1.345−2	1.96−1	4.58−1	5.76	0	1.34	8.53−1	5.10+1	8.25	8.09	4.27+2	1.35+2
	5.230−2	1.90−1	4.95−1	3.86	3.885−2	1.36	9.22−1	3.94+1	5.91	5.90	5.62+2	1.83+2
	1.023−1	1.82−1	5.34−1	2.42	8.885−2	1.27	1.08	2.66+1	4.07	4.05	6.72+2	2.21+2
	2.023−1	1.65−1	5.90−1	1.20	1.888−1	1.05	1.45	1.31+1	2.14	2.12	8.04+2	2.66+2
	3.023−1	1.48−1	6.30−1	7.22−1	2.888−1	8.48−1	1.83	7.51	1.27	1.26	8.86+2	2.94+2
	4.023−1	1.33−1	6.61−1	4.86−1	3.888−1	6.94−1	2.18	4.79	8.32−1	8.29−1	9.45+2	3.14+2
	5.023−1	1.20−1	6.86−1	3.50−1	4.888−1	5.75−1	2.51	3.30	5.84−1	5.83−1	9.91+2	3.30+2
	6.523−1	1.03−1	7.14−1	2.33−1	6.388−1	4.45−1	2.96	2.08	3.78−1	3.77−1	1.05+3	3.48+2
	9.023−1	8.15−2	7.49−1	1.36−1	8.888−1	3.05−1	3.62	1.14	2.15−1	2.15−1	1.11+3	3.70+2
	1.402	5.43−2	7.91−1	6.33−2	1.389	1.65−1	4.71	4.93−1	9.73−2	9.73−2	1.20+3	4.00+2
	2.402	2.88−2	8.30−1	2.37−2	2.389	6.88−2	6.27	1.72−1	3.57−2	3.57−2	1.31+3	4.35+2
	3.402	1.78−2	8.48−1	1.23−2	3.389	3.68−2	7.41	8.59−2	1.84−2	1.84−2	1.37+3	4.57+2
B^{3+}	1.142−2	2.07−1	4.72−1	4.73	0	1.47	9.46−1	4.92+1	6.34	6.32	4.59+2	1.48+2
	6.994−2	1.99−1	5.17−1	2.70	5.852−2	1.36	1.14	3.06+1	4.18	4.16	6.11+2	2.01+2
	1.199−1	1.90−1	5.47−1	1.83	1.085−1	1.23	1.32	2.10+1	3.01	3.00	6.91+2	2.28+2
	1.699−1	1.80−1	5.71−1	1.33	1.585−1	1.11	1.52	1.50+1	2.24	2.22	7.49+2	2.48+2
	2.699−1	1.60−1	6.10−1	7.97−1	2.585−1	9.07−1	1.89	8.55	1.34	1.34	8.32+2	2.76+2
	3.699−1	1.43−1	6.40−1	5.34−1	3.585−1	7.47−1	2.25	5.45	8.83−1	8.80−1	8.91+2	2.96+2

† 1.591−2 stands for 1.591×10^{-2}.

Table 2. (continued)

Ion	k_f^2/Z^2	$1^1S \rightarrow 2^3S$	$1^1S \rightarrow 2^1S$	$2^3S \rightarrow 2^1S$	k_f^2/Z^2	$1^1S \rightarrow 2^3P$	$1^1S \rightarrow 2^1P$	$2^3P \rightarrow 2^1P$	$2^3S \rightarrow 2^1P$	$2^1S \rightarrow 2^3P$	$2^3S \rightarrow 2^3P$	$2^1S \rightarrow 2^1P$
B^{3+}	4.699−1	1.29−1	6.65−1	3.83−1	4.585−1	6.23−1	2.58	3.75	6.23−1	6.21−1	9.35+2	3.11+2
	6.199−1	1.10−1	6.94−1	2.54−1	6.085−1	4.86−1	3.04	2.36	4.04−1	4.04−1	9.88+2	3.29+2
	8.699−1	8.67−2	7.30−1	1.48−1	8.585−1	3.37−1	3.72	1.30	2.31−1	2.31−1	1.05+3	3.50+2
	1.370	5.75−2	7.74−1	6.87−2	1.359	1.86−1	4.83	5.59−1	1.05−1	1.05−1	1.13+3	3.78+2
	2.370	3.05−2	8.17−1	2.56−2	2.359	7.85−2	6.44	1.94−1	3.86−2	3.86−2	1.23+3	4.10+2
	3.370	1.89−2	8.37−1	1.33−2	3.359	4.23−2	7.61	9.72−2	1.99−2	1.99−2	1.29+3	4.30+2
C^{4+}	9.857−3	2.18−1	4.81−1	4.16	0	1.49	1.04	4.57+1	5.42	5.39	4.70+2	1.53+2
	4.928−2	2.11−1	5.08−1	2.88	3.942−2	1.40	1.18	3.28+1	4.18	4.15	5.73+2	1.88+2
	9.928−2	2.00−1	5.37−1	1.95	8.942−2	1.27	1.37	2.24+1	3.04	3.02	6.60+2	2.18+2
	1.493−1	1.89−1	5.60−1	1.41	1.394−1	1.15	1.56	1.60+1	2.27	2.26	7.22+2	2.39+2
	2.493−1	1.68−1	5.98−1	8.42−1	2.394−1	9.37−1	1.94	9.12	1.37	1.37	8.07+2	2.68+2
	3.493−1	1.49−1	6.28−1	5.63−1	3.394−1	7.75−1	2.30	5.82	9.08−1	9.05−1	8.66+2	2.88+2
	4.493−1	1.34−1	6.53−1	4.04−1	4.394−1	6.49−1	2.63	4.01	6.43−1	6.41−1	9.11+2	3.03+2
	5.993−1	1.14−1	6.82−1	2.67−1	5.894−1	5.09−1	3.10	2.53	4.19−1	4.18−1	9.63+2	3.21+2
	8.493−1	8.98−2	7.18−1	1.56−1	8.394−1	3.55−1	3.78	1.40	2.40−1	2.40−1	1.02+3	3.41+2
	1.349	5.96−2	7.64−1	7.21−2	1.339	1.98−1	4.90	6.02−1	1.09−1	1.09−1	1.10+3	3.68+2
	2.349	3.17−2	8.09−1	2.69−2	2.339	8.47−2	6.54	2.09−1	4.04−2	4.04−2	1.20+3	3.99+2
	3.349	1.96−2	8.31−1	1.40−2	3.339	4.60−2	7.73	1.05−1	2.09−2	2.09−2	1.26+3	4.18+2
N^{5+}	8.651−3	2.25−1	4.85−1	3.81	0	1.49	1.12	4.26+1	4.89	4.86	4.75+2	1.55+2
	3.461−2	2.19−1	5.02−1	3.00	2.596−2	1.42	1.21	3.41+1	4.15	4.13	5.44+2	1.79+2
	8.461−2	2.06−1	5.30−1	2.02	7.596−2	1.29	1.41	2.32+1	3.04	3.03	6.40+2	2.11+2
	1.346−1	1.94−1	5.53−1	1.46	1.260−1	1.16	1.60	1.65+1	2.28	2.27	7.06+2	2.34+2
	2.346−1	1.72−1	5.90−1	8.73−1	2.260−1	9.54−1	1.98	9.46	1.39	1.38	7.95+2	2.64+2
	3.346−1	1.53−1	6.20−1	5.83−1	3.260−1	7.92−1	2.33	6.05	9.22−1	9.20−1	8.55+2	2.84+2
	4.346−1	1.37−1	6.44−1	4.18−1	4.260−1	6.65−1	2.67	4.18	6.55−1	6.54−1	9.00+2	3.00+2
	5.846−1	1.17−1	6.74−1	2.76−1	5.760−1	5.23−1	3.13	2.64	4.28−1	4.28−1	9.52+2	3.17+2
	8.346−1	9.19−2	7.10−1	1.61−1	8.260−1	3.68−1	3.82	1.46	2.47−1	2.46−1	1.01+3	3.37+2
	1.335	6.09−2	7.57−1	7.45−2	1.326	2.06−1	4.95	6.31−1	1.13−1	1.13−1	1.09+3	3.64+2
	2.335	3.24−2	8.04−1	2.78−2	2.326	8.90−2	6.60	2.19−1	4.16−2	4.16−2	1.18+3	3.94+2
	3.335	2.01−2	8.27−1	1.45−2	3.326	4.85−2	7.80	1.10−1	2.15−2	2.15−2	1.24+3	4.12+2

O^{6+}	7.699−3	2.29−1	4.88−1	3.58	0	1.48	1.18	4.01+1	4.55	4.52	4.76+2	1.56+2
	2.388−2	2.24−1	4.98−1	3.09	1.618−2	1.43	1.24	3.49+1	4.12	4.10	5.21+2	1.71+2
	7.388−2	2.11−1	5.25−1	2.08	6.618−2	1.30	1.44	2.36+1	3.04	3.02	6.27+2	2.07+2
	1.239−1	1.98−1	5.47−1	1.50	1.162−1	1.17	1.63	1.69+1	2.29	2.28	6.97+2	2.31+2
	2.239−1	1.76−1	5.84−1	8.94−1	2.162−1	9.65−1	2.01	9.68	1.40	1.39	7.89+2	2.62+2
	3.239−1	1.56−1	6.14−1	5.97−1	3.162−1	8.03−1	2.36	6.20	9.31−1	9.29−1	8.51+2	2.83+2
	4.239−1	1.39−1	6.38−1	4.27−1	4.162−1	6.76−1	2.70	4.29	6.63−1	6.62−1	8.97+2	2.98+2
	5.739−1	1.19−1	6.68−1	2.83−1	5.662−1	5.33−1	3.16	2.72	4.35−1	4.34−1	9.48+2	3.16+2
	8.239−1	9.33−2	7.05−1	1.65−1	8.162−1	3.76−1	3.85	1.51	2.51−1	2.51−1	1.01+3	3.36+2
	1.324	6.19−2	7.52−1	7.63−2	1.316	2.12−1	4.99	6.52−1	1.15−1	1.15−1	1.09+3	3.62+2
	2.324	3.30−2	8.00−1	2.85−2	2.316	9.22−2	6.65	2.27−1	4.25−2	4.25−2	1.18+3	3.92+2
	3.324	2.05−2	8.24−1	1.48−2	3.316	5.04−2	7.86	1.14−1	2.20−2	2.20−2	1.23+3	4.10+2
Ne^{8+}	6.293−3	2.32−1	4.90−1	3.28	0	1.45	1.27	3.65+1	4.13	4.11	4.77+2	1.56+2
	5.824−2	2.17−1	5.17−1	2.16	5.194−2	1.31	1.47	2.43+1	3.04	3.02	6.08+2	2.01+2
	1.082−1	2.04−1	5.39−1	1.55	1.019−1	1.19	1.67	1.73+1	2.29	2.29	6.88+2	2.28+2
	2.082−1	1.80−1	5.75−1	9.25−1	2.019−1	9.79−1	2.04	9.96	1.41	1.41	7.88+2	2.62+2
	3.082−1	1.59−1	6.04−1	6.16−1	3.019−1	8.17−1	2.40	6.41	9.44−1	9.42−1	8.52+2	2.83+2
	4.082−1	1.42−1	6.28−1	4.41−1	4.019−1	6.90−1	2.73	4.45	6.74−1	6.73−1	8.99+2	2.99+2
	5.582−1	1.21−1	6.58−1	2.92−1	5.519−1	5.47−1	3.19	2.83	4.44−1	4.43−1	9.51+2	3.17+2
	8.082−1	9.52−2	6.96−1	1.70−1	8.019−1	3.88−1	3.88	1.57	2.57−1	2.57−1	1.01+3	3.37+2
	1.308	6.32−2	7.44−1	7.88−2	1.302	2.21−1	5.02	6.81−1	1.18−1	1.18−1	1.09+3	3.63+2
	2.308	3.37−2	7.93−1	2.95−2	2.302	9.66−2	6.70	2.38−1	4.38−2	4.38−2	1.18+3	3.92+2
	3.308	2.10−2	8.18−1	1.53−2	3.302	5.31−2	7.91	1.19−1	2.27−2	2.27−2	1.23+3	4.09+2
Mg^{10+}	1.493−2	2.30−1	4.96−1	2.86	9.613−3	1.41	1.37	3.16+1	3.67	3.66	5.08+2	1.67+2
	4.793−2	2.21−1	5.12−1	2.21	4.261−2	1.32	1.50	2.45+1	3.03	3.02	5.97+2	1.97+2
	9.793−2	2.07−1	5.33−1	1.59	9.261−2	1.19	1.69	1.75+1	2.30	2.29	6.85+2	2.27+2
	1.979−1	1.82−1	5.69−1	9.44−1	1.926−1	9.86−1	2.06	1.01+1	1.42	1.41	7.93+2	2.63+2
	2.979−1	1.62−1	5.98−1	6.29−1	2.926−1	8.25−1	2.42	6.53	9.51−1	9.50−1	8.60+2	2.86+2
	3.979−1	1.44−1	6.22−1	4.50−1	3.926−1	6.98−1	2.75	4.54	6.81−1	6.80−1	9.08+2	3.02+2
	5.479−1	1.23−1	6.52−1	2.97−1	5.426−1	5.55−1	3.22	2.89	4.49−1	4.49−1	9.61+2	3.20+2
	7.979−1	9.64−2	6.90−1	1.74−1	7.926−1	3.95−1	3.91	1.61	2.61−1	2.61−1	1.02+3	3.40+2
	1.298	6.40−2	7.39−1	8.04−2	1.293	2.26−1	5.05	7.01−1	1.20−1	1.20−1	1.10+3	3.66+2
	2.298	3.42−2	7.89−1	3.01−2	2.293	9.95−2	6.72	2.45−1	4.46−2	4.46−2	1.18+3	3.94+2
	3.298	2.13−2	8.15−1	1.57−2	3.293	5.48−2	7.95	1.23−1	2.31−2	2.31−2	1.23+3	4.12+2

Table 2. (continued)

Ion	k_f^2/Z^2	$1^1S \rightarrow 2^3S$	$1^1S \rightarrow 2^1S$	$2^3S \rightarrow 2^1S$	k_f^2/Z^2	$1^1S \rightarrow 2^3P$	$1^1S \rightarrow 2^1P$	$2^3P \rightarrow 2^1P$	$2^3S \rightarrow 2^1P$	$2^1S \rightarrow 2^3P$	$2^3S \rightarrow 2^3P$	$2^1S \rightarrow 2^1P$	L_m†
Si^{12+}	1.470−2	2.31−1	4.97−1	2.74	1.011−2	1.39	1.41	3.00+1	3.51	3.50	5.12+2	1.68+2	
	4.070−2	2.23−1	5.09−1	2.24	3.611−2	1.32	1.52	2.47+1	3.02	3.01	5.89+2	1.94+2	
	9.070−2	2.09−1	5.30−1	1.61	8.611−2	1.20	1.71	1.76+1	2.29	2.29	6.87+2	2.27+2	
	1.907−1	1.84−1	5.65−1	9.55−1	1.861−1	9.90−1	2.08	1.02+1	1.42	1.42	8.01+2	2.66+2	
	2.907−1	1.63−1	5.94−1	6.36−1	2.861−1	8.29−1	2.43	6.60	9.56−1	9.54−1	8.70+2	2.89+2	
	3.907−1	1.45−1	6.18−1	4.55−1	3.861−1	7.03−1	2.77	4.59	6.85−1	6.84−1	9.19+2	3.06+2	
	5.407−1	1.24−1	6.48−1	3.01−1	5.361−1	5.60−1	3.23	2.93	4.53−1	4.52−1	9.73+2	3.24+2	
	7.907−1	9.72−2	6.86−1	1.76−1	7.861−1	4.00−1	3.92	1.64	2.63−1	2.63−1	1.03+3	3.44+2	
	1.291	6.46−2	7.36−1	8.15−2	1.286	2.30−1	5.06	7.14−1	1.21−1	1.21−1	1.11+3	3.70+2	
	2.291	3.46−2	7.87−1	3.05−2	2.286	1.02−1	6.75	2.50−1	4.52−2	4.52−2	1.19+3	3.98+2	
	3.291	2.16−2	8.12−1	1.59−2	3.286	5.60−2	7.97	1.26−1	2.34−2	2.34−2	1.25+3	4.15+2	
Ca^{18+}	1.342−2	2.31−1	4.97−1	2.55	1.015−2	1.36	1.49	2.76+1	3.26	3.25	5.22+2	1.72+2	
	2.842−2	2.27−1	5.04−1	2.28	2.515−2	1.32	1.55	2.47+1	3.00	2.99	5.78+2	1.91+2	
	7.842−2	2.12−1	5.24−1	1.64	7.515−2	1.20	1.75	1.77+1	2.28	2.28	7.00+2	2.32+2	
	1.784−1	1.86−1	5.58−1	9.72−1	1.752−1	9.94−1	2.12	1.03+1	1.42	1.42	8.30+2	2.76+2	
	2.784−1	1.65−1	5.87−1	6.48−1	2.752−1	8.35−1	2.47	6.69	9.60−1	9.59−1	9.04+2	3.01+2	
	3.784−1	1.47−1	6.12−1	4.64−1	3.752−1	7.10−1	2.80	4.67	6.90−1	6.90−1	9.56+2	3.18+2	
	5.284−1	1.26−1	6.42−1	3.07−1	5.252−1	5.67−1	3.27	3.00	4.58−1	4.57−1	1.01+3	3.37+2	
	7.784−1	9.86−2	6.80−1	1.80−1	7.752−1	4.07−1	3.96	1.68	2.67−1	2.67−1	1.07+3	3.57+2	
	1.278	6.55−2	7.31−1	8.33−2	1.275	2.35−1	5.10	7.35−1	1.24−1	1.24−1	1.15+3	3.83+2	
	2.278	3.51−2	7.83−1	3.13−2	2.275	1.05−1	6.79	2.59−1	4.62−2	4.62−2	1.23+3	4.11+2	
	3.278	2.20−2	8.09−1	1.63−2	3.275	5.81−2	8.02	1.30−1	2.39−2	2.39−2	1.28+3	4.27+2	
Fe^{24+}	1.183−2	2.31−1	4.96−1	2.48	9.295−3	1.35	1.53	2.65+1	3.15	3.15	5.28+2	1.74+2	
	3.183−2	2.25−1	5.05−1	2.14	2.929−2	1.30	1.61	2.29+1	2.82	2.81	6.10+2	2.02+2	
	7.183−2	2.14−1	5.21−1	1.65	6.929−2	1.20	1.77	1.77+1	2.27	2.27	7.17+2	2.37+2	
	1.718−1	1.88−1	5.55−1	9.80−1	1.693−1	9.96−1	2.14	1.03+1	1.42	1.42	8.58+2	2.85+2	
	2.718−1	1.66−1	5.84−1	6.54−1	2.693−1	8.38−1	2.49	6.72	9.62−1	9.61−1	9.36+2	3.11+2	
	3.718−1	1.48−1	6.08−1	4.68−1	3.693−1	7.13−1	2.82	4.71	6.93−1	6.92−1	9.89+2	3.29+2	
	5.218−1	1.26−1	6.39−1	3.10−1	5.193−1	5.71−1	3.28	3.03	4.60−1	4.60−1	1.05+3	3.48+2	
	7.718−1	9.93−2	6.77−1	1.81−1	7.693−1	4.11−1	3.97	1.70	2.69−1	2.69−1	1.11+3	3.69+2	

	1.272	6.60−2	7.28−1	8.43−2	1.269	2.39−1	5.12	7.47−1	1.25−1	1.25−1	1.18+3	3.95+2	
	2.272	3.54−2	7.81−1	3.17−2	2.269	1.07−1	6.81	2.63−1	4.67−2	4.67−2	1.27+3	4.22+2	
	3.272	2.22−2	8.08−1	1.65−2	3.269	5.92−2	8.05	1.32−1	2.42−2	2.42−2	1.32+3	4.39+2	
$Z=\infty$	0	2.33−1	4.90−1	2.34	0	1.32	1.64	2.42+1	2.93	2.93	1.72+2	5.52+1	6
	5.000−2	2.18−1	5.09−1	1.68	5.000−2	1.20	1.83	1.75+1	2.24	2.24	2.20+2	7.17+1	11
	1.500−1	1.91−1	5.43−1	1.00	1.500−1	9.98−1	2.20	1.03+1	1.41	1.41	2.39+2	7.88+1	12
	2.500−1	1.70−1	5.72−1	6.69−1	2.500−1	8.44−1	2.55	6.81	9.64−1	9.64−1	2.30+2	7.60+1	12
	3.500−1	1.51−1	5.97−1	4.81−1	3.500−1	7.22−1	2.88	4.80	6.99−1	6.99−1	2.35+2	7.79+1	13
	5.000−1	1.29−1	6.27−1	3.20−1	5.000−1	5.81−1	3.34	3.11	4.67−1	4.67−1	2.20+2	7.32+1	13
	7.500−1	1.01−1	6.67−1	1.87−1	7.500−1	4.22−1	4.03	1.76	2.75−1	2.75−1	1.99+2	6.62+1	13
	1.250	6.76−2	7.19−1	8.75−2	1.250	2.48−1	5.17	7.82−1	1.28−1	1.28−1	1.95+2	6.48+1	15
	2.250	3.64−2	7.74−1	3.30−2	2.250	1.12−1	6.87	2.78−1	4.83−2	4.83−2	2.08+2	6.92+1	20
	3.250	2.28−2	8.02−1	1.72−2	3.250	6.29−2	8.12	1.40−1	2.51−2	2.51−2	2.22+2	7.40+1	25

† For $Z=\infty$ $2^3S\rightarrow 2^3P$ and $2^1S\rightarrow 2^1P$, the sum of partial collision strengths up to $L=L_m$ is given.

logarithmically (see Burgess *et al* 1970) since the energy levels are degenerate in this approximation. The collision strengths given for these two transitions are those for the partial sum from $L=0$ to L_m. In the infinite Z limit the off-diagonal ρ-matrix elements of the CEDW2 approximation (see I) differ only by spin factors and by factors arising from the operation of the Pauli exclusion principle (see III, equations (2.18*a*), (2.18*b*)) from the R- (reactance) matrix elements of Burgess *et al* (1970) against which they were spot checked.

As Z increases relativistic effects begin to become important and so LS coupling begins to break down (see e.g. Pradhan 1983a). This can be expected mainly to affect the $1^1S_0 \rightarrow 2^3P_1$, $2^3P_1 \rightarrow 2^1P_1$, $2^1S_0 \rightarrow 2^3P_1$ and $2^3S_1 \rightarrow 2^1P_1$ transitions, which can only take place through electron exchange in LS coupling but in an intermediate-coupling scheme can also take place directly via spin-orbit interaction, etc. Jones (1974) has made a detailed comparison between the two coupling schemes. From his work we estimate that the errors in our results for $\Omega(1^1S_0 \rightarrow 2^3P_1)$ and, on summing over fine structure, $\Omega(2^3P \rightarrow 2^1P)$, due to the neglect of relativistic effects, will be about 25% for Fe^{24+}, about 10% for Ca^{18+} and negligible for the other ions considered. Jones (1974) found that for the $2^1S \rightarrow 2^3P$ transition in Fe^{24+} $\Omega_{IC} \simeq 8\Omega_{LS}$. We therefore suggest that our results for $\Omega(2^1S \rightarrow 2^3P)$ and $\Omega(2^3S \rightarrow 2^1P)$ be used with caution, particularly for ions above Mg^{10+}. For all other transitions relativistic corrections can be expected to be negligible for the ions considered here.

The near-threshold $1^1S \rightarrow 2^1P$ partial collision strengths are now being used in a calculation of rate coefficients for the dielectronic recombination of He-like ions.

Acknowledgments

I wish to thank Dr Alan Burgess and Dr John Tully for some helpful discussions. This work was supported by a SERC award.

References

Badnell N R 1983a *J. Phys. B: At. Mol. Phys.* **16** 3263-78
—— 1983b *Cambridge Department of Applied Mathematics and Theoretical Physics Report* DAMTP/AA/-1000-NRB
—— 1984 *J. Phys. B: At. Mol. Phys.* **17** 4013-32
Burgess A, Hummer D G and Tully J A 1970 *Phil. Trans. R. Soc.* A **266** 225-79
Burke P G, Berrington K A and Sukumar C V 1981 *J. Phys. B: At. Mol. Phys.* **14** 289-305
Henry R J W 1981 *Phys. Rep.* **68** 1-91
Jones M 1974 *Mon. Not. R. Astron. Soc.* **169** 211-27
Kingston A E and Tayal S S 1983 *J. Phys. B: At. Mol. Phys.* **16** 3465-78
Nakazaki S and Hashino T 1982 *J. Phys. B: At. Mol. Phys.* **15** 2295-305
Powell M J D 1981 *Approximation Theory and Methods* (Cambridge: Cambridge University Press)
Pradhan A K 1983a *Phys. Rev.* A **28** 2113-27
—— 1983b *Phys. Rev.* A **28** 2128-36
Pradhan A K, Norcross D W and Hummer D G 1981a *Phys. Rev.* A **23** 619-31
—— 1981b *Astrophys. J.* **246** 1031-9
Steenman-Clark L and Faucher P 1984 *J. Phys. B: At. Mol. Phys.* **17** 73-81
Tayal S S and Kingston A E 1984a *J. Phys. B: At. Mol. Phys.* **17** L145-9
—— 1984b *J. Phys. B: At. Mol. Phys.* **17** 1383-90
Trefftz E 1983 *J. Phys. B: At. Mol. Phys.* **16** 1247-51
Tully J A 1980 *J. Phys. B: At. Mol. Phys.* **13** 3023-34
Weiss A W 1967 *J. Res. NBS* **71A** 163-8
van Wyngaarden W L, Bhadra K and Henry R J W 1979 *Phys. Rev.* A **20** 1409-17